Quantum Many-Body Dynamics in Optomechanical Arrays

Max Ludwig[1,*] and Florian Marquardt[1,2]

[1]*Institute for Theoretical Physics, Universität Erlangen-Nürnberg, Staudtstraße 7, 91058 Erlangen, Germany*
[2]*Max-Planck-Institute for the Science of Light, Günther-Scharowsky-Straße 1/Bau 24, 91058 Erlangen, Germany*

(Received 1 August 2012; revised manuscript received 30 May 2013; published 16 August 2013)

We study the nonlinear driven dissipative quantum dynamics of an array of optomechanical systems. At each site of such an array, a localized mechanical mode interacts with a laser-driven cavity mode via radiation pressure, and both photons and phonons can hop between neighboring sites. The competition between coherent interaction and dissipation gives rise to a rich phase diagram characterizing the optical and mechanical many-body states. For weak intercellular coupling, the mechanical motion at different sites is incoherent due to the influence of quantum noise. When increasing the coupling strength, however, we observe a transition towards a regime of phase-coherent mechanical oscillations. We employ a Gutzwiller ansatz as well as semiclassical Langevin equations on finite lattices, and we propose a realistic experimental implementation in optomechanical crystals.

DOI: 10.1103/PhysRevLett.111.073603 PACS numbers: 42.50.Wk

Introduction.—Recent experimental progress has brought optomechanical systems into the quantum regime: A single mechanical mode interacting with a laser-driven cavity field has been cooled to the ground state [1,2]. Several of these setups, in particular optomechanical crystals, offer the potential to be scaled up to form optomechanical arrays. Applications of such arrays for quantum information processing [3,4] have been proposed. Given these developments, one is led to explore quantum many-body effects in optomechanical arrays. In this work, we analyze the nonlinear photon and phonon dynamics in a homogeneous two-dimensional optomechanical array. In contrast to earlier works [3–6], here we study the array's quantum dynamics beyond a quadratic Hamiltonian. To tackle the nonequilibrium many-body problem of this nonlinear dissipative system, we employ a mean-field approach for the collective dynamics. First, we discuss photon statistics in the array, in particular, how the photon blockade effect [7] is altered in the presence of intercellular coupling. The main part of the article focuses on the transition of the collective mechanical motion from an incoherent state (due to quantum noise) to an ordered state with phase-coherent mechanical oscillations. For these dynamics, the dissipative effects induced by the optical modes play a crucial role. On the one hand, they allow the mechanical modes to settle into self-induced oscillations [8] once the optomechanical amplification rate exceeds the intrinsic mechanical damping. On the other hand, the fundamental quantum noise (e.g., cavity shot noise) diffuses the mechanical phases and prevents the mechanical modes from synchronizing. This interplay leads to an elaborate phase diagram characterizing the transition. We develop a semiclassical model to describe the effective dynamics of the mechanical phases and to study the system on finite lattices.

While true long-range order is prohibited for a two-dimensional system with continuous symmetry, at least for equilibrium systems, a Beresinskii-Kosterlitz-Thouless transition towards a state with quasi-long-range order is possible. The ordered mechanical phase thus resembles the superfluid phase in two-dimensional cold atomic gases [9] or Josephson junction arrays [10]. Notably, optomechanical arrays combine the tunability of optical systems with the robustness and durability of an integrated solid-state device. Other driven dissipative systems that have been studied with regard to phase transitions recently include cold atomic gases [11–14], nonlinear cavity arrays [15,16] and optical fibers [17]. In a very recent work and along the lines of [11], the preparation of long-range order for photonic modes was proposed using the linear dissipative effects in an optomechanical array [5]. Our work adds the novel aspect of a mechanical transition to the studies of driven dissipative many-body systems.

Model.—We study the collective quantum dynamics of a two-dimensional homogeneous array of optomechanical cells (Fig. 1). Each of these cells consists of a mechanical

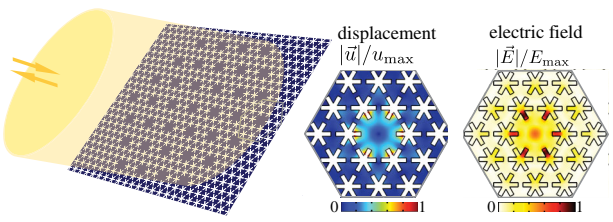

FIG. 1 (color online). Example implementation of an optomechanical array: A two-dimensional snowflake optomechanical crystal [38,39] supports localized optical and mechanical modes around defect cavities. Here, we propose arranging them in a superstructure, forming the array. The insets show electric field $\vec{E}$ and displacement field $\vec{u}$ of an isolated defect cavity (obtained from finite element simulations). Due to the finite overlap between modes of neighboring sites [29], photons and phonons can hop through the array, see Eq. (2). A wide laser beam drives the optical modes of the array continuously and the reflected light is read out.

mode and a laser driven optical mode that interact via the radiation pressure coupling at a rate g_0 ($\hbar = 1$):

$$\hat{H}_{\mathrm{om},j} = -\Delta \hat{a}_j^\dagger \hat{a}_j + \Omega \hat{b}_j^\dagger \hat{b}_j - g_0(\hat{b}_j^\dagger + \hat{b}_j)\hat{a}_j^\dagger \hat{a}_j + \alpha_L(\hat{a}_j^\dagger + \hat{a}_j). \quad (1)$$

The mechanical mode ($\hat{b}_j$) is characterized by a frequency Ω. The cavity mode ($\hat{a}_j$) is transformed into the frame rotating at the laser frequency ($\Delta = \omega_{\mathrm{laser}} - \omega_{\mathrm{cav}}$) and driven at the rate α_L. In the most general case, both photons and phonons can tunnel between neighboring sites $\langle ij \rangle$ at rates J/z and K/z, where z denotes the coordination number. The full Hamiltonian of the array is given by $\hat{H} = \sum_j \hat{H}_{\mathrm{om},j} + \hat{H}_{\mathrm{int}}$, with

$$\hat{H}_{\mathrm{int}} = -\frac{J}{z}\sum_{\langle i,j \rangle}(\hat{a}_i^\dagger \hat{a}_j + \hat{a}_i \hat{a}_j^\dagger) - \frac{K}{z}\sum_{\langle i,j \rangle}(\hat{b}_i^\dagger \hat{b}_j + \hat{b}_i \hat{b}_j^\dagger). \quad (2)$$

To bring this many-body problem into a treatable form, we apply the Gutzwiller ansatz $\hat{A}_i^\dagger \hat{A}_j \approx \langle \hat{A}_i^\dagger \rangle \hat{A}_j + \hat{A}_i^\dagger \langle \hat{A}_j \rangle - \langle \hat{A}_i^\dagger \rangle \langle \hat{A}_j \rangle$ to Eq. (2). The accuracy of this approximation improves if the number of neighboring sites z increases. For identical cells, the index j can be dropped and the Hamiltonian reduces to a sum of independent contributions, each of which is described by

$$\hat{H}_{\mathrm{mf}} = \hat{H}_{\mathrm{om}} - J(\hat{a}^\dagger \langle \hat{a} \rangle + \hat{a} \langle \hat{a}^\dagger \rangle) - K(\hat{b}^\dagger \langle \hat{b} \rangle + \hat{b} \langle \hat{b}^\dagger \rangle). \quad (3)$$

Hence, a Lindblad master equation for the single cell density matrix $\hat{\rho}$, $d\hat{\rho}/dt = -i[\hat{H}_{\mathrm{mf}}, \hat{\rho}] + \kappa \mathcal{D}[\hat{a}]\hat{\rho} + \Gamma \mathcal{D}[\hat{b}]\hat{\rho}$ can be employed. The Lindblad terms $\mathcal{D}[\hat{A}]\hat{\rho} = \hat{A}\,\hat{\rho}\,\hat{A}^\dagger - \hat{A}^\dagger \hat{A}\,\hat{\rho}/2 - \hat{\rho}\hat{A}^\dagger \hat{A}/2$ take into account photon decay at a rate κ and mechanical dissipation (here assumed due to a zero temperature bath) at a rate Γ.

Photon statistics.—Recently, it was shown that the effect of the photon blockade [7] can appear in a single optomechanical cell: The interaction with the mechanical mode induces an optical nonlinearity of strength g_0^2/Ω [7,18] and the presence of a single photon can hinder other photons from entering the cavity. To observe this effect, the nonlinearity must be comparable to the cavity decay rate, i.e., $g_0^2/\Omega \gtrsim \kappa$, and the laser drive weak ($\alpha_L \ll \kappa$) [7,19].

To study nonclassical effects in the photon statistics, we analyze the steady-state photon correlation function $g^{(2)}(\tau) = \langle \hat{a}^\dagger(t)\hat{a}^\dagger(t+\tau)\hat{a}(t+\tau)\hat{a}(t) \rangle / \langle \hat{a}(t)^\dagger \hat{a}(t) \rangle^2$ [20] at equal times ($\tau = 0$). Here (Fig. 2), we probe the influence of the collective dynamics by varying the optical coupling strength J, while keeping the mechanical coupling K zero for clarity. We note that, when increasing J, the optical resonance effectively shifts: $\Delta \longrightarrow \Delta + J$. To keep the photon number fixed while increasing J, the detuning has to be adapted [21]. In this setting, we observe that the interaction between the cells suppresses antibunching [Fig. 2(b)]. The photon blockade is lost if the intercellular coupling becomes larger than the effective nonlinearity, $2J \gtrsim g_0^2/\Omega$. Above this value, the photon statistics shows bunching, and ultimately reaches Poissonian statistics for large couplings.

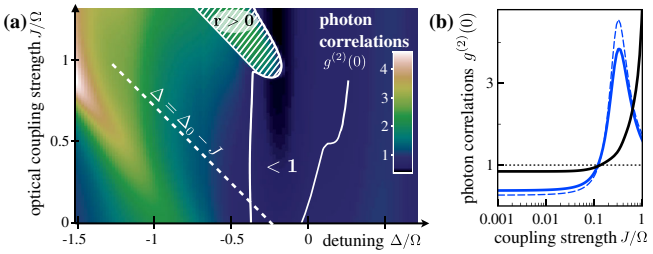

FIG. 2 (color online). Loss of the photon blockade for increasing optical coupling in an array of optomechanical cavities. (a) The equal time photon correlation function shows antibunching ($g^{(2)}(0) < 1$) and bunching ($g^{(2)}(0) > 1$) as a function of detuning Δ and optical coupling strength J. The smallest values of $g^{(2)}(0)$ are found for a detuning $\Delta_0 = -g_0^2/\Omega$. (b) When increasing the coupling J while keeping the intracavity photon number constant, i.e., along the dashed line in panel (a), the photon blockade is lost (black solid line). For a smaller driving power (blue solid line, $\alpha_L = 5 \times 10^{-5}\kappa$), anti-bunching is more pronounced and the behavior is comparable to that of a nonlinear cavity (dashed line). The hatched area in (a) outlines a region where a transition towards coherent mechanical oscillations has set in. $\kappa = 0.3\ \Omega$, $\alpha_L = 0.65\kappa$, $g_0 = 0.5\ \Omega$, $\Gamma = 0.074\ \Omega$.

Similar physics has recently been analyzed for coupled qubit-cavity arrays, [21]. For large coupling strengths, though, Fig. 2(a) reveals signs of the collective mechanical motion (hatched area). There we observe the correlation function to oscillate (at the mechanical frequency) and to show bunching. We will now investigate this effect.

Collective mechanical quantum effects.—To describe the collective mechanical motion of the array, we focus on the case of purely mechanical intercellular coupling ($K > 0$, $J = 0$) for simplicity. Note, though, that the effect is also observable for optically coupled arrays, as discussed above.

As our main result, Figs. 3(a) and 3(d) show the sharp transition between incoherent self-oscillations and a phase-coherent collective mechanical state as a function of both laser detuning Δ and coupling strength K: In the regime of self-induced oscillations, the phonon number $\langle \hat{b}^\dagger \hat{b} \rangle$ reaches a finite value. Yet, the expectation value $\langle \hat{b} \rangle$ remains small and constant in time. When increasing the intercellular coupling, though, $\langle \hat{b} \rangle$ suddenly starts oscillating and reaches a steady state

$$\langle \hat{b} \rangle(t) = \bar{b} + re^{-i\Omega_{\mathrm{eff}}t}. \quad (4)$$

Here, we introduced the mechanical coherence r and the oscillation frequency Ω_{eff}, which is shifted by the optical fields and the intercellular coupling, cf. Eq. (6).

Our more detailed analysis (see below) indicates that this transition results from the competition between the fundamental quantum noise of the system and the tendency of phase locking between the coupled nonlinear oscillators. Below threshold, the quantum noise from the phonon bath and the optical fields diffuses the mechanical phases at different sites and drives the mechanical motion

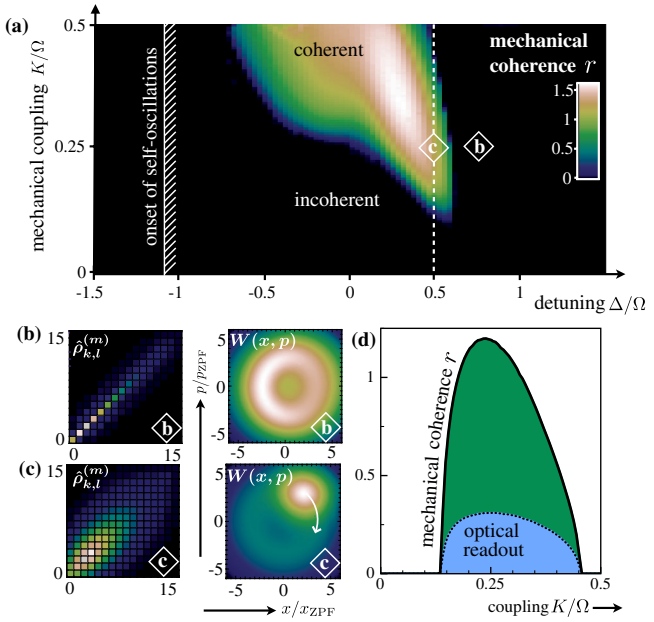

FIG. 3 (color online). Transition from the incoherent to the synchronized (coherent) phase: (a) Mechanical coherence r [Eq. (4)] as a function of laser detuning Δ and mechanical coupling K. At weak coupling, the self-oscillations are incoherent, $r = 0$, due to quantum noise. When increasing the coupling strength, the systems shows a sharp transition towards the ordered regime, where the mechanical oscillations are phase coherent, $r > 0$. (b), (c) Modulus of the density matrix elements (in Fock space) and Wigner density of the collective mechanical state in the incoherent (b) and the coherent regime (c), as marked in (a). (d) Mechanical coherence r as a function of coupling strength K along the dashed line in (a). The dotted line shows the optical readout of coherence, i.e., the oscillating component of the photon number $\langle \hat{a}^\dagger \hat{a} \rangle$, proportional to the intensity of the reflected beam and thus directly accessible in experiment. $g_0 = \kappa = 0.3\ \Omega$, $\alpha_L = 1.1\kappa$, $\Gamma = 0.074\ \Omega$.

into an incoherent mixed state. The reduced density matrix $\hat{\rho}^{(m)}$ is predominantly occupied on the diagonal, see Fig. 3(b), and the Wigner distribution, $W(x,p) = (1/\pi\hbar) \times \int_{-\infty}^{\infty} \langle x - y | \hat{\rho}^{(m)} | x + y \rangle e^{2ipy/\hbar} dy$, has a ringlike shape, reflecting the fact that the mechanical phase is undetermined [22,23]. Above threshold, the mechanical motion at different sites becomes phase locked, and the coherence parameter r reaches a finite value. The emergence of coherence also becomes apparent from the off-diagonal elements of $\hat{\rho}^{(m)}$ [Fig. 3(c)]. The corresponding Wigner function assumes the shape of a coherent state with a definite phase oscillating in phase space. Thus, this transition spontaneously breaks the time-translation symmetry. In a two-dimensional implementation, true long range order is excluded, but the coherence between different sites is expected to decay as a power law with distance. We also note that this transition is the quantum mechanical analogon of classical synchronization, which was studied for optomechanical systems in [24–26]. An important difference is, though, that the classical nonlinear dynamics was analyzed for an inhomogeneous (with disordered mechanical frequencies) system in the absence of noise [24–26], while in our case disorder is only introduced via fundamental quantum noise. Quantum synchronization has also been discussed in the context of linear oscillators [27] and nonlinear cavities [28] recently.

The laser detuning determines both the strength of the self-oscillations and the influence of the cavity shot noise on the mechanical motion. It turns out that the diffusion of the mechanical phases is pronounced close to the onset of self-oscillations and at the mechanical sideband [29]. As we will show below, even the coherent coupling between the mechanical phases (ultimately leading to synchronization) is tunable via the laser frequency. As a result, the synchronization threshold depends nontrivially on the detuning parameter Δ, see Fig. 3(a).

Langevin dynamics on finite lattices.—In order to gain further insight into the coupling and decoherence mechanisms as well as effects of geometry and dimensionality, we analyze the semi-classical Langevin equations of the full optomechanical array:

$$\dot{\beta}_i = \left(-i\Omega - \frac{\Gamma}{2}\right)\beta_i + ig_0|\alpha_i|^2 + i\frac{K}{z}\sum_{\langle ij \rangle}\beta_j + \sqrt{\frac{\Gamma}{2}}\xi_\beta$$

$$\dot{\alpha}_i = \left(i\Delta + ig_0(\beta_i + \beta_i^*) - \frac{\kappa}{2}\right)\alpha_i - i\alpha_L + \sqrt{\frac{\kappa}{2}}\xi_\alpha. \qquad (5)$$

The fluctuating noise forces $\xi_{\sigma=\alpha,\beta}(t)$ mimic the effects of the zero temperature phonon bath and the cavity shot noise, respectively. They are independent at each site and obey $\langle \xi_\sigma \rangle = 0$ and $\langle \xi_\sigma(t)\xi_\sigma^*(t') \rangle = \delta(t - t')$. In this context, $\langle \ldots \rangle$ denotes the average over different realizations of the stochastic terms. This Langevin approach is equivalent to the truncated Wigner approximation (see [30] for a review), and it has shown good qualitative agreement with the full quantum dynamics for a single optomechanical cell [22,31]. It allows us to treat the effects of quantum fluctuations at all wavelengths on the spatial phase correlations via numerical simulations. At this point, a full quantum treatment for sufficiently large systems remains a challenging problem for future studies.

First, we study the onset of quasi-long-range order in a finite system. To this end we evaluate the correlations $C(d = |i - j|) = \langle e^{i\varphi_i} e^{-i\varphi_j} \rangle$, where $e^{i\varphi_i} = \beta_i/|\beta_i|$. Numerical calculations on a 30×30 square lattice [see Fig. 4(a)] indicate that for weak intercellular coupling the mechanical phases at different sites are uncorrelated even for small distances d. When increasing the coupling strength, however, the mechanical motion becomes correlated over the whole array with only a slow decrease with distance. The coupling threshold, here defined by setting a lower bound of $C(14) > 0.01$, varies with the coordination number, see Fig. 4(b). Within the mean-field approximation, i.e., for a lattice with global coupling of all sites, fluctuations between neighboring sites and hence the threshold value are underestimated. The coupling threshold grows with the quantum parameter [22], i.e., the ratio of optomechanical coupling and cavity decay rate, g_0/κ, see Fig. 4(c): For $g_0 \approx \kappa$, single

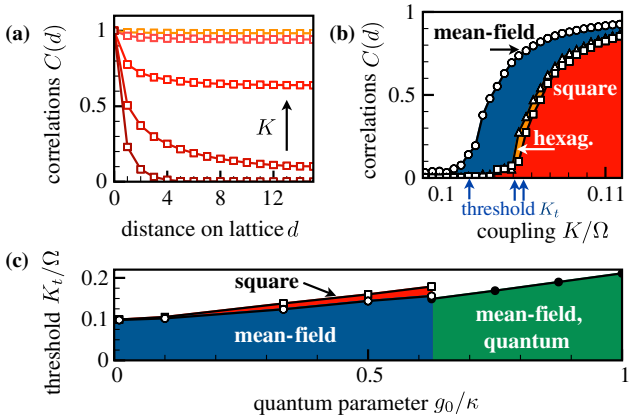

FIG. 4 (color online). Langevin dynamics on finite lattices: (a) Correlations $C(d = |i - j|) = |\langle e^{i\varphi_i} e^{-i\varphi_j}\rangle|$ in a 30×30 optomechanical array. Quasi-long-range order sets in for sufficiently large coupling strengths. $K = \{0.09, 0.105, 0.107, 0.12, 0.15\}\ \Omega$. (b) Correlations over a distance of $d = 14$ as a function of mechanical coupling strength K for a square lattice ($z = 4$, squares), a hexagonal lattice ($z = 6$, triangles) slightly below the mean-field result (circles). (c) Coupling threshold as a function of quantum parameter g_0/κ (squares: square lattice, empty (filled) circles: semiclassical (quantum) mean-field approach). $\Delta + g_0^2/\Omega = 0.34$, $g_0 = 0.1\kappa$ in (a),(b), $g_0\alpha_L = 0.33\kappa$ in (c), other parameters as in Fig. 3.

photons and phonons interact strongly and quantum fluctuations hamper synchronization.

Synchronization threshold.—For an analytical approach, the complexity of the Langevin equations can be reduced by integrating out the dynamics of the optical modes and the mechanical amplitudes and by going back to the mean-field approximation [29]. The resulting equation describes the coupling of the mechanical phase on a single site, φ, to a mean field Ψ:

$$\dot{\varphi} = -\Omega(\bar{A}) + KR\cos(\Psi - \varphi) + K_1 R\sin(\Psi - \varphi) + \sqrt{2D_\varphi}\xi_\varphi + \mathcal{O}(R^2). \quad (6)$$

Here, the order parameter is defined as $\langle e^{i\varphi_j}\rangle \equiv Re^{i\Psi}$. The rate $K_1 = (d\Omega - K/2)K/\gamma$ determines the coupling of phases mediated by slow amplitude modulations between neighboring sites. These beat modes couple back to the phase dynamics via the amplitude dependent optical spring effect, $\Omega(\bar{A}) + d\Omega(A - \bar{A})/\bar{A}$, where $d\Omega = \bar{A}(d\Omega/dA)|_{A=\bar{A}}$, and the bare mechanical coupling K, leading to two opposing terms in K_1. Here, $\bar{A}$ denotes the steady state mechanical amplitude and γ the amplitude decay rate set by the optical field. The fluctuating noise force $\sim\xi_\varphi$ comprises the effects of mechanical fluctuations and radiation pressure noise and is characterized by a diffusion constant D_φ [29,31].

Equation (6) reveals the close connection to the Kuramoto model [32] and the two-dimensional xy model. In the incoherent regime, the order parameter R is zero and the phase fluctuates freely. In the coherent regime, the restoring force $\sim K_1 R$ leads the phase φ towards a fixed relation with Ψ. The cosine term only renormalizes the oscillation frequency. This statement can be clarified by a linear stability analysis, see [29,33]. It turns out that the incoherent phase becomes unstable for

$$K_1 = 2D_\varphi, \quad (7)$$

defining the threshold of the transition. Moreover, if K_1 becomes negative, no stable phase synchronization is possible. This situation arises if $d\Omega < 0$, or for large intercellular coupling rates $K > 2d\Omega$, see Fig. 3(d).

Experimental prospects.—We note that observation of the mechanical phase transition does *not* require single photon strong coupling ($g_0 \gtrsim \kappa$): The quantum fluctuations of the light field will dominate over thermal fluctuations as long as $4g_0^2|\alpha|^2/\kappa > k_B T/Q$. This is essentially the condition for ground-state cooling, which has been achieved using high-Q mechanical resonators and cryogenic cooling [1,2], see Table I. In contrast, the photon-blockade effect (Fig. 2) requires low temperatures T and $g_0^2 \gtrsim \Omega\kappa$, or at least, in a slightly modified setup [35,36], $g_0 \gtrsim \kappa$. While still challenging, optomechanical systems are approaching this regime [37].

Microfabricated optomechanical systems such as microresonators (e.g., [34]), optomechanical crystals (e.g., [2]) or microwave-based setups (e.g., [1]) lend themselves to extensions to optomechanical arrays. Here, we focus on optomechanical crystals, which are well suited due to their extremely small mode volumes. The properties of two-dimensional optomechanical crystals have been analyzed in [38]. The finite overlap of the evanescent tails of adjacent localized modes [29] results in a coupling of the form of Eq. (2), in analogy to the tight-binding description of electronic states in solids. Sufficiently strong optical and mechanical hopping rates are feasible, see [24] for one-dimensional and [29] for two-dimensional structures. The simultaneous optical driving of many cells may be realized by a single broad laser beam irradiating the slab, see Fig. 1. Alternatively, similar physics may be observed for many mechanical modes coupling to one extended

TABLE I. Parameters of optomechanical systems [1,2,34]: Temperature of phonon bath T, strength of mechanical fluctuations $\Gamma n_{\rm th} \approx k_B T/Q$, strength of cavity shot noise $\Gamma_{\rm opt} \approx 4g_0^2|\bar{\alpha}|^2/\kappa$, quantum parameter g_0/κ and approximate size L.

Setup	$T[K]$	$\Gamma n_{\rm th}/\Omega$	$\Gamma_{\rm opt}/\Omega$	g_0/κ	$L[\mu m]$
Microwave based	25 mK	10^{-4}	7×10^{-3}	10^{-3}	$\sim$100
Optomech. crystal	20 K	10^{-3}	4×10^{-3}	2×10^{-3}	$\sim$4
Microtoroid	650 mK	7×10^{-2}	6×10^{-2}	5×10^{-4}	$\sim$30

in-plane optical mode [6,24,25] (thereby effectively realizing global coupling).

The transition towards the synchronized phase can be detected by probing the light reflected from the optomechanical array and measuring the component oscillating at the mechanical frequency, see Fig. 3(d). To read out correlations between individual sites, the intensities of individual defect cavities may be analyzed [29], for example by evanescently coupling them to tapered fibers or waveguides.

We expect the transition to be robust against disorder [24]. One may also study the formation of vortices and other topological defects induced by engineered irregularities and periodic variations, and explore various different lattice structures or the possibility of other order phases (e.g., antiferromagnetic order). Thus, optomechanical arrays provide a novel, integrated, and tunable platform for studies of quantum many body effects.

The authors would like to thank Oskar Painter and Björn Kubala for valuable discussions. This work was supported by the DFG Emmy-Noether program, an ERC starting grant, the DARPA/MTO ORCHID program, and the ITN network cQOM.

*max.ludwig@physik.uni-erlangen.de

[1] J. D. Teufel, T. Donner, D. Li, J. W. Harlow, M. S. Allman, K. Cicak, A. J. Sirois, J. D. Whittaker, K. W. Lehnert, and R. W. Simmonds, Nature (London) **475**, 359 (2011).
[2] J. Chan, T. P. M. Alegre, A. H. Safavi-Naeini, J. T. Hill, A. Krause, S. Groblacher, M. Aspelmeyer, and O. Painter, Nature (London) **478**, 89 (2011).
[3] D. E. Chang, A. H. Safavi-Naeini, M. Hafezi, and O. Painter, New J. Phys. **13**, 023003 (2011).
[4] M. Schmidt, M. Ludwig, and F. Marquardt, New J. Phys. **14**, 125005 (2012).
[5] A. Tomadin, S. Diehl, M. D. Lukin, P. Rabl, and P. Zoller, Phys. Rev. A **86**, 033821 (2012).
[6] A. Xuereb, C. Genes, and A. Dantan, Phys. Rev. Lett. **109**, 223601 (2012).
[7] P. Rabl, Phys. Rev. Lett. **107**, 063601 (2011).
[8] T. Carmon, H. Rokhsari, L. Yang, T. J. Kippenberg, and K. J. Vahala, Phys. Rev. Lett. **94**, 223902 (2005); F. Marquardt, J. G. E. Harris, and S. M. Girvin, *ibid.* **96**, 103901 (2006); C. Metzger, M. Ludwig, C. Neuenhahn, A. Ortlieb, I. Favero, K. Karrai, and F. Marquardt, *ibid.* **101**, 133903 (2008); Q. Lin, J. Rosenberg, X. Jiang, K. J. Vahala, and O. Painter, *ibid.* **103**, 103601 (2009); M. Bagheri, M. Poot, M. Li, W. P. H. Pernice, and H. X. Tang, Nat. Nanotechnol. **6**, 726 (2011).
[9] Z. Hadzibabic, P. Krüger, M. Cheneau, B. Battelier, and J. Dalibard, Nature (London) **441**, 1118 (2006).
[10] R. Fazio and H. van der Zant, Phys. Rep. **355**, 235 (2001).
[11] S. Diehl, A. Micheli, A. Kantian, B. Kraus, H. P. Buchler, and P. Zoller, Nat. Phys. **4**, 878 (2008).
[12] D. Nagy, G. Kónya, G. Szirmai, and P. Domokos, Phys. Rev. Lett. **104**, 130401 (2010).
[13] K. Baumann, C. Guerlin, F. Brennecke, and T. Esslinger, Nature (London) **464**, 1301 (2010).
[14] T. E. Lee, H. Häffner, and M. C. Cross, Phys. Rev. A **84**, 031402 (2011).
[15] M. J. Hartmann, F. G. S. L. Brandão, and M. B. Plenio, Nat. Phys. **2**, 849 (2006).
[16] A. D. Greentree, C. Tahan, J. H. Cole, and L. C. L. Hollenberg, Nat. Phys. **2**, 856 (2006).
[17] D. E. Chang, V. Gritsev, G. Morigi, V. Vuletić, M. D. Lukin, and E. A. Demler, Nat. Phys. **4**, 884 (2008).
[18] A. Nunnenkamp, K. Børkje, and S. M. Girvin, Phys. Rev. Lett. **107**, 063602 (2011).
[19] A. Kronwald, M. Ludwig, and F. Marquardt, Phys. Rev. A **87**, 013847 (2013).
[20] L. Mandel and E. Wolf, *Optical Coherence and Quantum Optics* (Cambridge University Press, Cambridge, England, 1995).
[21] F. Nissen, S. Schmidt, M. Biondi, G. Blatter, H. E. Türeci, and J. Keeling, Phys. Rev. Lett. **108**, 233603 (2012).
[22] M. Ludwig, B. Kubala, and F. Marquardt, New J. Phys. **10**, 095013 (2008).
[23] J. Qian, A. A. Clerk, K. Hammerer, and F. Marquardt, Phys. Rev. Lett. **109**, 253601 (2012).
[24] G. Heinrich, M. Ludwig, J. Qian, B. Kubala, and F. Marquardt, Phys. Rev. Lett. **107**, 043603 (2011).
[25] C. A. Holmes, C. P. Meaney, and G. J. Milburn, Phys. Rev. E **85**, 066203 (2012).
[26] M. Zhang, G. S. Wiederhecker, S. Manipatruni, A. Barnard, P. McEuen, and M. Lipson, Phys. Rev. Lett. **109**, 233906 (2012).
[27] G. L. Giorgi, F. Galve, G. Manzano, P. Colet, and R. Zambrini, Phys. Rev. A **85**, 052101 (2012).
[28] T. E. Lee and M. C. Cross, arXiv:1209.0742.
[29] See Supplemental Material at http://link.aps.org/supplemental/10.1103/PhysRevLett.111.073603 for details on the effective phase equations, possible experimental implementations and the numerical methods used.
[30] A. Polkovnikov, Ann. Phys. (Amsterdam) **325**, 1790 (2010).
[31] D. A. Rodrigues and A. D. Armour, Phys. Rev. Lett. **104**, 053601 (2010).
[32] Y. Kuramoto, Prog. Theor. Phys. Suppl. **79**, 223 (1984).
[33] S. H. Strogatz and R. E. Mirollo, J. Stat. Phys. **63**, 613 (1991).
[34] E. Verhagen, S. Deleglise, S. Weis, A. Schliesser, and T. J. Kippenberg, Nature (London) **482**, 63 (2012).
[35] K. Stannigel, P. Komar, S. J. M. Habraken, S. D. Bennett, M. D. Lukin, P. Zoller, and P. Rabl, Phys. Rev. Lett. **109**, 013603 (2012).
[36] M. Ludwig, A. H. Safavi-Naeini, O. Painter, and F. Marquardt, Phys. Rev. Lett. **109**, 063601 (2012).
[37] J. Chan, A. H. Safavi-Naeini, J. T. Hill, S. Meenehan, and O. Painter, Appl. Phys. Lett. **101**, 081115 (2012).
[38] A. H. Safavi-Naeini and O. Painter, Opt. Express **18**, 14 926 (2010).
[39] A. H. Safavi-Naeini and O. Painter, New J. Phys. **13**, 013017 (2011).